

# Sensors & Diagnostics

rsc.li/sensors

The Royal Society of Chemistry is the world's leading chemistry community. Through our high impact journals and publications we connect the world with the chemical sciences and invest the profits back into the chemistry community.

## IN THIS ISSUE

ISSN 2635-0998 CODEN SDEIAR 3(8) 1227-1360 (2024)



### Cover

See Saimon M. Silva *et al.*, pp. 1234–1246.  
Image reproduced by permission of Ahmad Ridzwan Rahmat from *Sens. Diagn.*, 2024, 3, 1234.



### Inside cover

See Denis Svehkarev *et al.*, pp. 1253–1262.  
Image reproduced by permission of Denis Svehkarev from *Sens. Diagn.*, 2024, 3, 1253.

## PERSPECTIVE

1234

### A holistic pathway to biosensor translation

Laena D'Alton, Dênio Emanuel Pires Souto, Chamindie Punyadeera, Brian Abbey, Nicolas H. Voelcker, Conor Hogan and Saimon M. Silva\*

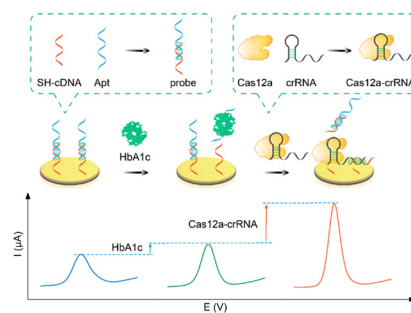


## COMMUNICATION

1247

### A CRISPR-amplified label-free electrochemical aptasensor for the sensitive detection of HbA1c

Jianfeng Ma, Youwei Zheng, Yaoyao Xie, Dan Zhu, Lianhui Wang\* and Shao Su\*



# Royal Society of Chemistry approved training courses

Explore your options.  
Develop your skills.  
Discover learning  
that suits you.

**Courses in the classroom,  
the lab, or online**

Find something for every  
stage of your professional  
development. Search our  
database by:

- subject area
- location
- event type
- skill level

Members **get at least 10% off**

Visit [rsc.li/cpd-training](https://rsc.li/cpd-training)

**SAVE  
10%**

Registered charity number: 207890



# Fast and accurate identification of pathogenic bacteria using excitation–emission spectroscopy and machine learning

The diagram illustrates a neural network architecture. On the left, a 2D heatmap labeled "Excitation-emission spectra" shows a bright yellow-green region on a dark blue background. An arrow points from this heatmap to a neural network diagram. The neural network consists of three layers: an input layer with 3 green circles, a hidden layer with 4 red squares, and an output layer with 2 blue diamonds. Lines connect each node in one layer to every node in the next layer. To the right of the neural network, the text "Species classification" is followed by "85.8%" and "98.3%" in large blue font. Below this, the text "Gram status classification" is shown.

# Synthesis and fluorescence properties of 2'-benzyloxy flavone—a dual probe for selective detection of picric acid and pH sensing

The figure illustrates the chemical structures and sensing mechanisms of the PA and Fluorophore. The PA (Protonic Absorbance) structure is shown as a complex molecule with a central core and multiple substituents. The Fluorophore structure is shown as a simpler molecule with a central core and a single substituent. The fluorescence quenching mechanism is depicted as a reaction scheme where the PA and Fluorophore interact, leading to a decrease in fluorescence intensity. The fluorescence intensity vs. wavelength graph shows two peaks: a red peak for the PA and a blue peak for the Fluorophore. The pH sensing mechanism is shown as a reaction scheme where the Fluorophore reacts with H<sup>+</sup> to form a protonated species, which is then quenched by the PA.

## Ultra-sensitive detection of PFASs using surface enhanced Raman scattering and machine learning: a promising approach for environmental analysis

# A highly selective chromo-fluorogenic probe for specific detection of sarin gas simulant diethylchlorophosphate in liquid and vapor phases

TSB

TSB + DCP

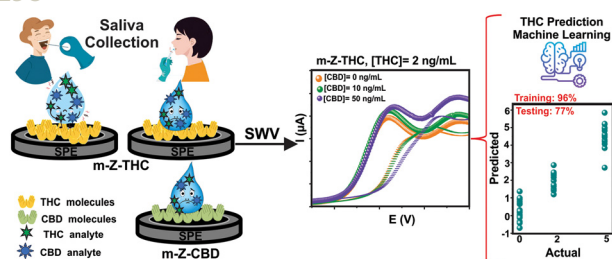
Paper strips

Gas phase detection

- ✓ Chromo-fluorogenic detection
- ✓  $\mu\text{M}$  detection limit
- ✓ Real sample analysis

## PAPERS

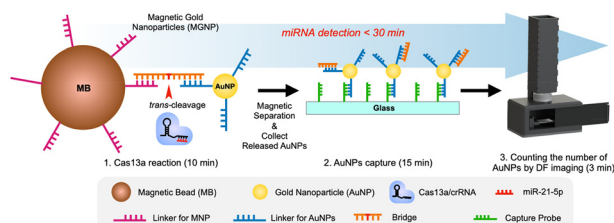
1298



### Ultra-low dual detection of tetrahydrocannabinol and cannabidiol in saliva based on electrochemical sensing and machine learning: overcoming cross-interferences and saliva-to-saliva variations

Greter A. Ortega, Herlys Viltres, Hoda Mozaffari, Syed Rahin Ahmed, Seshasai Srinivasan\* and Amin Reza Rajabzadeh\*

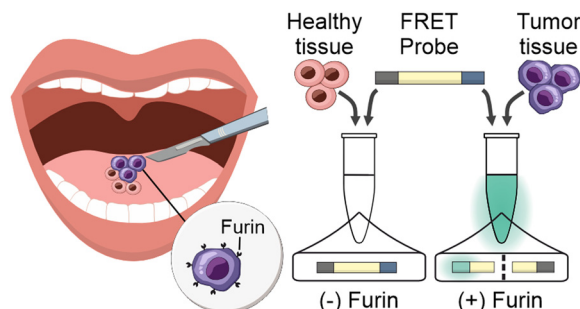
1310



### CRISPR/Cas13a-assisted amplification-free miRNA biosensor via dark-field imaging and magnetic gold nanoparticles

Jae-Jun Kim, Jae-Sang Hong, Hyunho Kim, Moonhyun Choi, Ursula Winter, Hakho Lee and Hyungsoon Im\*

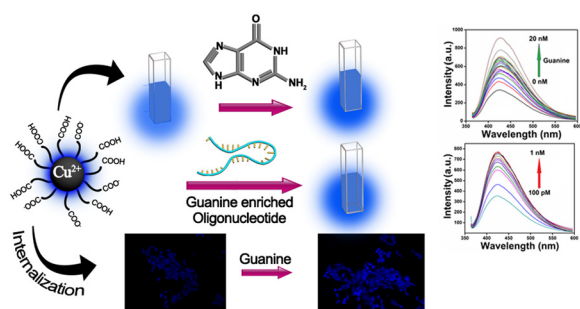
1319



### Visually distinguishing between tumor tissue and healthy tissue within ten minutes using proteolytic probes

Debora Reinhardt, Björn ter Mors, Marc D. Driessen, Marcus Gutmann, Julian Faber, Lukas Haug, Anna-Maria Faber, Anna Herrmann, Prisca Hamm, Tessa Lühmann, Christian Linz\* and Lorenz Meinel\*

1329



### Cu<sup>2+</sup>-integrated carbon dots as an efficient bioprobe for the selective sensing of guanine nucleobase

Monalisa Chowdhury, Debolina Basu and Prasanta Kumar Das\*

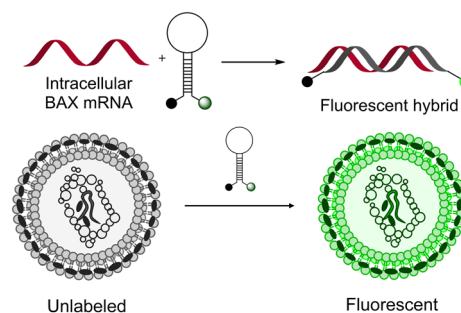


## PAPERS

1344

### Microfluidic measurement of intracellular mRNA with a molecular beacon probe towards point-of-care radiation triage

Xin Meng, Kechun Wen, Jingyang Zhao, Yaru Han, Shanaz A. Gandhi, Salan P. Kaur, David J. Brenner, Helen C. Turner, Sally A. Amundson\* and Qiao Lin\*



1353

### DNA walker coupled with nicking endonuclease for sensitive electrochemical detection of saxitoxin

Yiwei Liu, Shumin Feng, Ruoxi Zhong, Yuanchang Peng, Guoyuan Mu, Jiayi Bai, Wei Chen\* and Zhan Qu\*

